BIOCHEMICAL PHARMACOLOGY 73 (2007) 491–503

available at www.sciencedirect.com

ScienceDirect

journal homepage: www.elsevier.com/locate/biochempharm

Peripheral-type benzodiazepine receptor overexpression and knockdown in human breast cancer cells indicate its prominent role in tumor cell proliferation

Wenping Li [a], *Matthew J. Hardwick* [a], *Dean Rosenthal* [a,b], *Martine Culty* [a], *Vassilios Papadopoulos* [a,b,*]

[a] *Department of Biochemistry & Molecular and Cellular Biology, Georgetown University Medical Center, Washington, DC 20057, USA*
[b] *The Lombardi Comprehensive Cancer Center, Georgetown University Medical Center, Washington, DC 20057, USA*

ARTICLE INFO

Article history:
Received 7 July 2006
Accepted 24 October 2006

Keywords:
MCF-7
MDA-MB-231
RNA interference
Cell cycle
$p21^{WAF/CIP1}$
p53
Caspase-3

ABSTRACT

The peripheral-type benzodiazepine receptor (PBR), an 18-kDa high affinity drug and cholesterol binding protein, is expressed at high levels in various cancers. Its expression is positively correlated with aggressive metastatic behavior in human breast cancer cells. To determine the role of PBR in tumor progression, two human mammary carcinoma cell lines were utilized: the non-aggressive MCF-7 cell line, which expresses extremely low PBR levels, and the highly aggressive MDA-MB-231 cell line, which has much higher PBR levels. We have generated stably transfected lines of the tetracycline-repressible MCF-7 cell line (MCF-7 Tet-Off) with inducible human PBR cDNA. Induction of PBR expression in MCF-7 Tet-Off cells increased PBR ligand binding and cell proliferation. Transfection of MDA-MB-231 cells with multiple siRNAs complementary to PBR (PBR–siRNAs) led to different levels of PBR mRNA knockdown. Lentiviral-mediated PBR RNA interference in MDA-MB-231 cells decreased PBR levels by 50%. Decreased PBR expression was associated with cell cycle arrest at G2 phase, decreased cell proliferation, and significant increases in the protein levels of the cyclin-dependent kinase inhibitor $p21^{WAF/CIP1}$. These changes were accompanied by p53 activation seen as increased p53 phosphorylation (Ser15). In parallel, increased proteolytic activation of caspase-3 was also observed. Taken together these results suggest that PBR protein expression is directly involved in regulating cell survival and proliferation in human breast cancer cells by influencing signaling mechanisms involved in cell cycle control and apoptosis.

1. Introduction

Breast cancer is one of the most common neoplasms and the leading cause of cancer-related deaths in women in most developing countries [1]. In breast cancer, tumor progression occurs *via* a multi-step process in which normal cells gradually acquire more malignant phenotypes, including the ability to invade tissues and form distal metastases. These metastases are the primary cause of mortality. Considering that the first step of tumor progression is increased cell survival and/or proliferation, it can be envisaged that tumorigenesis and malignancy are related to the proliferative potential of tumor cells. Therefore, it is important to identify the cellular

* *Corresponding author at*: Department of Biochemistry & Molecular and Cellular Biology, Georgetown University Medical Center, 3900 Reservoir Road NW, Washington, DC 20057, USA. Tel.: +1 202 687 8991; fax: +1 202 687 7855.
E-mail address: papadopv@georgetown.edu (V. Papadopoulos).
0006-2952/$ – see front matter
doi:10.1016/j.bcp.2006.10.025

components that are involved in enhancing such proliferative potential.

The peripheral-type benzodiazepine receptor (PBR) may be one cellular component that is involved in regulating cell proliferation. Conversely, its dysregulation could be involved in the increased proliferation of cancer cells. PBR was identified because of its ability to bind the benzodiazepine diazepam in tissues that do not express the central benzodiazepine receptor [2,3]. PBR is an 18-kDa protein that is abundant in steroid-synthesizing tissues, such as gonads, adrenal gland, placenta and brain [2,3]. PBR resides primarily in the outer mitochondrial membrane where it regulates the transport of cholesterol to the mitochondrial inner membrane. This transport process is the rate-determining step in steroidogenesis [2]. Recent studies have shown that PBR is a high-affinity cholesterol-binding protein [4,5]. Considering its widespread distribution [2,3] and its ability to bind cholesterol [4,5], PBR might affect cholesterol compartmentalization and membrane biogenesis, which are events involved in cell proliferation and death. Indeed, PBR has been shown to be important in mitochondrial respiration [6] and cell survival [7–11]. Additionally, PBR has been implicated as a therapeutic target for cancer, as well as cardiovascular and neurological diseases [12,13].

Numerous studies conducted during the last decade have indicated that PBR may also play a role in carcinogenesis. The PBR receptor is highly expressed in testicular and adrenocortical cells and in brain gliomas. PBR drug ligands (e.g., benzodiazepines) have been shown to regulate the proliferation of such cells [14]. PBR expression has been correlated with the high metastatic potential of human astrocytomas and other types of human brain tumors [15,16]. PBR ligands have also been shown to influence the proliferation of various tumors, such as gliomas and lymphomas [17–22]. Increased densities of PBR binding sites have been found in colonic adenocarcinoma [23–25], ovarian carcinoma [26,27], and in human brain gliomas, as compared to normal tissue [27,28]. Also, recent studies have indicated that antitumor drugs that act *via* PBR (e.g., PBR ligand-drug conjugates) may be useful in treating pancreatic and brain tumors [29,30]. Pharmacological concentrations of high-affinity PBR drug ligands can induce apoptosis in various cancer cell lines [31–36], and that PBR ligands may act as chemosensitizing agents for the treatment of human neoplasms [37,38].

In previous studies, we examined the expression, characteristics, localization, and function of PBR in a battery of human breast cancer cell lines that differed in their invasive and chemotactic potentials [31]. PBR ligand-binding and PBR mRNA levels were significantly higher in highly aggressive cell lines, such as MDA-MB-231, than in non-aggressive cell lines, such as MCF-7. This difference may be due, at least in part, to PBR gene amplification [39,40]. PBR was also expressed at high levels in aggressive metastatic human breast tumor biopsies, compared to normal breast tissue [27,31,41]. In further studies, we found that the ability of aggressive breast tumor cells to form tumors *in vivo* might depend on the amount of PBR present in the cells. Furthermore, exposure of MDA-MB-231 cells to high-affinity PBR drug ligands increased the incorporation of bromodeoxyuridine (BrdU) into the cells, indicating that PBR plays a role in regulating cell proliferation in this aggressive cancer cell line [40].

2. Materials and methods

2.1. Materials

MCF-7 and MDA-MB-231 human breast cancer cell lines were obtained from the Lombardi Comprehensive Cancer Center, Georgetown University Medical Center. The 293T/17 cell line was from American Type Culture Collection (ATCC, Manassas, VA). Dulbecco's modified Eagle medium (DMEM) and Fetal Bovine Serum (FBS) were purchased from Cellgro (Mediatech, Inc., Herndon, VA). Penicillin and streptomycin were obtained from Invitrogen Corporation (Carlsbad, CA). The tetracycline-repressible MCF-7 cell line, designated "MCF-7 Tet-Off" was from BD Biosciences Clontech (Palo Alto, CA). Tet-Approved FBS, pBI-EGFP expression vector, and pTK-Hyg vector were obtained from Clontech. Plasticware was supplied by Corning (Corning, NJ). Hygromycin and doxycycline (Dox) were obtained from Sigma Aldrich (St. Louis, MO). [^{3}H]PK 11195 [1-(2-chlorophenyl)-*N*-methyl-*N*-(1-methylpropyl)-3-isoquinoline-carboxamide; specific activity, 85.5 Ci/mmol] was obtained from NEN Life Science Products (Boston, MA). Bio-Rad Protein Assay Kit was obtained from Bio-Rad Laboratories (Hercules, CA). Poly-D-lysine slides were supplied by Becton Dickinson Labware (Bedford, MA). Anti-vimentin antiserum was from Chemicon International, Inc. (Temecula, CA). Omnicon 3800 Tumor Colony Analyzer was purchased from Imaging Products International, Inc. (Chantilly, VA). Small interfering RNAs (siRNAs) consisting of 21 nucleotides were synthesized by Dharmacon Research (Lafayette, CO) using 2′-ACE protection chemistry. Oligofectamine reagent, Opti-MEM, Lipofectamine, and Plus™ Reagent were from Invitrogen. Qiagen RNeasy Mini kit and RNase-free DNase were obtained from Qiagen (Valencia, CA). ABI PRISM 7700 Sequence Detection System, TaqMan Reverse Transcription Reagents, and SYBR Green PCR Master Mix were purchased from Applied Biosystems (Foster City, CA). All DNA primers were synthesized by MWG-BIOTECH Inc. (High Point, NC). BrdU Cell Proliferation ELISA was from Roche Molecular Biochemicals (Indianapolis, IN). Double-promoter pFIV-H1/U6-copGFP™ siRNA Cloning and Expression Vector, and pFIV-PACK Packaging Plasmid Mix were obtained from System Biosciences (Mountain View, CA). Coulter Counter Multisizer 3 was purchased from Beckman Coulter, Inc. (Fullerton, CA). PBR antibody was an affinity-purified anti-peptide rabbit polyclonal antiserum raised against the conserved amino acid sequence 9–27 as described [5]. Antibodies to p21$^{WAF1/CIP1}$, CyclinA, CyclinB1, Retinoblastoma protein (Rb) were obtained from BD Biosciences (San Jose, CA). Anti-glyceraldehyde 3-phosphate dehydrogenase (anti-GAPDH) was obtained from Trevigen Inc. (Gaithersburg, MD). Antibodies to cleaved caspase-3 and Phospho-p53 (Ser15) were obtained from Cell Signalling (Beverly, MA). Proliferating cell nuclear antigen (PCNA) antibody was purchase from Santa Cruz Biotechnology (Santa Cruz, CA). Enhanced chemiluminescence (ECL) kit was purchased from Amersham Biosciences (Arlington Heights, IL). Prism v3.0 software was obtained from GraphPad Inc. (San

Diego, CA). Other reagents were obtained from appropriate commercial sources.

2.2. Cell culture

MCF-7 and MDA-MB-231 human breast cancer cell lines were grown in Dulbecco's modified Eagle medium (DMEM) supplemented with 10% fetal bovine serum (FBS) plus 100 U/ml penicillin and 10 μg/ml streptomycin. The commercially available tetracycline-repressible MCF-7 cell line, designated "MCF-7 Tet-Off" was used for stably transfecting human PBR cDNA under the control of the TET REs. MCF-7 Tet-Off mock-transfected cells (designated "MOM") and MCF-7 Tet-Off-Induced expression of PBR cells (designated "MIP") were maintained in DMEM supplemented with 10% Tet-Approved FBS. Stable MIP transfectants were later termed "MIP1" and "MIP2".

2.3. Stable transfection of MCF-7 Tet-Off cells with PBR cDNA

Approximately 8×10^5 MCF-7 Tet-Off cells were co-transfected with 40 μg of either the pBI-EGFP vector alone (mock-transfected MCF-7 Tet-Off, or MOM cells), or with the vector plus the full-length human PBR cDNA (MIP cells) and 2 μg of the pTK-Hyg vector via electroporation (220 V, 950 μF). pBI-EGFP is a bi-directional expression vector possessing both the enhanced green fluorescent protein (EGFP) cDNA and a multi-cloning sequence under the expression of a bi-directional minimal cytomegalovirus promoter containing a Tet-responsive element. Thus, pBI-EGFP permits the simultaneous expression of the PBR gene and EGFP. The pTK-Hyg vector confers hygromycin resistance and served as a negative selection marker in this study. After electroporation, cells were plated in DMEM supplemented with 10% Tet System Approved FBS without antibiotics for 2 days at 37 °C, 6% CO_2. The cells were then maintained in DMEM, 10% Tet System Approved FBS supplemented with 100 μg/ml hygromycin and 1 μg/ml doxycycline (Dox). After several weeks, colonies over 2 mm in size were isolated and amplified in DMEM, 10% Tet System Approved FBS supplemented with 100 μg/ml hygromycin and 1 μg/ml Dox.

2.4. Doxycycline-induced reduction of EGFP expression

Selected stably-transfected MIP clones, MIP1 and MIP2, were plated onto 96-well plates at a concentration of 5000 cells/well and allowed to grow for 3 days in DMEM supplemented with 10% Tet System Approved FBS in the presence of 0, 0.0001, 0.01, or 1.0 μg/ml Dox. In this gene expression system, the Tet-controlled transcriptional transactivator activates transcription in the absence of the inducer (Dox). After incubation, cells were washed twice with PBS, and EGFP fluorescence was determined at 485 nm excitation and 510 nm emission.

2.5. Radioligand binding assays

Cells were scraped from 150-mm culture dishes into 6 ml of phosphate buffered saline (PBS), dispersed by trituration, and assayed for protein concentration. [^{3}H]PK 11195 binding to samples representing 40 μg of protein from cell suspensions was determined as previously described [31]. Specific [^{3}H] PK 11195 binding was analyzed using the iterative non-linear curve-fitting program Radlig 4.0 (KELL suite, Biosoft, Cambridge, UK). Protein levels were measured according to Bradford [42] using the Bio-Rad Protein Assay Kit and bovine serum albumin as the standard.

2.6. Immunochemical determination of vimentin

Approximately 20,000 cells per well of MCF-7 Tet-Off, MIP1 and MIP2 cells lines and 5000 cells per well for MDA-MB-231 were plated onto poly-D-lysine slides and incubated overnight at 37 °C, 6% CO_2. Cells were then fixed in 10% formaldehyde for 10 min at room temperature. After washing thoroughly with distilled H_2O, anti-vimentin, diluted 1:3 in PBS supplemented with 10% FBS, was added to each well. Samples were incubated overnight at 4 °C. After thoroughly rinsing the slides in PBS, horseradish peroxidase-conjugated goat anti-mouse secondary antibody, diluted 1:1000 in PBS supplemented with 10% FBS, was added to each well. Immunoreactivity was revealed as previously described [40].

2.7. Crystal violet cell proliferation assay

Cells grown to confluency were trypsinized and plated on 96-well plates at a concentration of 5000 cells/well. Cells were maintained in DMEM supplemented with 10% Tet System Approved FBS. Dox was added to the designated samples at a concentration of 1 μg/ml. Medium were changed every 2 days. At the specified time points, cells were fixed and stained in Crystal Violet solution (100 μl/well of 0.5% Crystal Violet, 25% methanol) for 10 min at room temperature. Plates were then thoroughly washed in 1× PBS, dried overnight, resuspended in citrate buffer and read at 600 nm.

2.8. Soft agar colony formation assay

For this assay, 5000 cells were suspended in 1.5 ml top agar (0.35% agar, DMEM supplemented with 10% Tet System Approved FBS) and plated on 1.5 ml base agar (0.5% agar, DMEM plus 10% Tet System Approved FBS) in one well of a 6-well plate. Cells were incubated at 37 °C, 6% CO_2 for 14 days. On day 2, a thin layer of liquid DMEM supplemented with 10% Tet System Approved FBS was added to each well. At the end of the assay, colony formation was determined by reading each plate using an Omnicon 3800 Tumor Colony Analyzer.

2.9. Preparation of siRNAs

Small interfering RNAs (siRNAs) consisting of 21 nucleotides were synthesized using 2′-ACE protection chemistry and used as previously described [43]. In brief, the siRNA strands were deprotected according to the manufacturer's instructions, mixed in equimolar ratios and annealed at 60 °C for 45 min and at ambient temperature for 30 min. The GeneBank accession number for human PBR is gi 21536444. SiRNA duplexes with the following sense and antisense sequences were used: PBR 361 siRNA targeting human PBR exon 3,5′-CUGGGCAUGGCCCCCCAUCdTdT-3′ (sense), 5′-GAUGGGGGGC-CAUGCCCAGdTdT-3′ (antisense); PBR 537 siRNA targeting

human PBR exon 4,5′-CUACUGCGUAUGGCGGGAC-dTdT3′ (sense), 5′-GUCCCGCCAUACGCAGUAGdTdT-3′ (antisense); PBR 548 siRNA targeting human PBR exon 4,5′-CCAUGGCUGG-CAUGGGGGAdTdT-3′ (sense), 5′-UCCCCCAUGCCAGCCAUGGdT dT-3′ (antisense); Scrambled siRNA, 5′-GGCUACUAUGCGGC-GACUGdTdT-3′ (sense), 5′-CAGUCGCCGCAUAGUAGCCdTdT-3′ (antisense). PBR 361, 537 and 548 siRNAs correspond to PBR coding regions and scrambled siRNA served as the control. Sequences for the siRNAs were selected as follows: 75 bases downstream from the start codon the first AA dimer (base 202–203 in gi 21536444) was located and the next 19 nucleotides were selected and the percentage of guanosines and cytidines (G/C content) of the (N19)TT 21-base sequence was calculated as 76.2%. Ideally, the G/C content should be ~50% (less than 70% and greater than 30%). Since this sequence does not meet the criterion, the search continues downstream to the next AA dimer until this condition is met. Each 21-base sequence was subjected to a BLAST-search (NCBI Database) against EST libraries to ensure that only one gene was targeted. The base-pairing region for each siRNA was selected carefully to avoid chance complementarity to an unrelated mRNA. PBR 361 siRNA targets human PBR 5′-ctgggcatggccccccatc-3′ (G/C content 66.7%) following aa (base 361–362 in gi 21536444); PBR 537 siRNA targets human PBR 5′-ctactgcgtatggcgggac-3′ (G/C content 57.1%) following aa (base 537–538 in gi 21536444); and PBR 548 siRNA targets human PBR 5′-ccatggctggcatggggga-3′ (G/C content 61.9%) following aa (base 558–559 in gi 21536444). The most efficient silencing was obtained with siRNA duplexes composed of 21-nt sense and 21-nt antisense strands, paired in a manner to have a 19-nucleotide duplex region and a 2-nucleotide overhang at each 3′-terminus. Therefore, the dTdT 3′-overhang of the antisense sequences is complementary to the target mRNA but the symmetrical dTdT 3′-overhang of the sense siRNA oligo does not need to correspond to the mRNA.

2.10. Transfection of MDA-MB-231 human breast cancer cells with PBR–siRNA duplexes

A single transfection of siRNA duplexes was performed using the Oligofectamine reagent. The cells were assayed for silencing later. Cells had been seeded the previous day in DMEM supplemented with 10% FBS in the absence of antibiotics. The siRNA duplex was mixed with Opti-MEM. In a separate tube, the Oligofectamine reagent was mixed with Opti-MEM and incubated for 10 min at room temperature. The two solutions were combined, gently mixed by inversion, incubated for 20 min at room temperature, and then the resulting siRNA-Oligofectamine was added to cells that were cultured at 30–50% confluency. Twenty-four hours later, fresh DMEM supplemented with 30% FBS was added to transfected cells to obtain a final concentration of 10% FBS.

2.11. Real-time quantitative PCR (Q-PCR)

Following incubation with or without siRNA, cells were washed three times with 1× PBS (pH 7.4). Total RNA was isolated using the Qiagen RNeasy Mini kit according to the manufacturer's specifications. Total RNA was submitted to On-Column DNase I digestion with RNase-free DNase in order to remove genomic DNA contamination. Q-PCR was performed using the ABI PRISM 7700 Sequence Detection System as previously described [44]. Briefly, total RNA was reverse-transcribed into cDNA using TaqMan Reverse Transcription Reagents, and the resulting cDNA was then processed for amplification of the PBR gene using specific primers. Each sample was run in triplicate. Direct detection of the PCR products was achieved by measuring the increase in fluorescence caused by the binding of SYBR® Green I Dye to double-stranded (ds) DNA. The Comparative C_T Method was used to analyze the data. The amount of PBR mRNA expression was normalized to the endogenous reference (18S rRNA). The following forward and reverse primers (5′–3′) were used for Q-PCR: TCCCAGTAAGTGCGGGTCAT and CCAATCGG-TAGTAGCGACGG for 18S rRNA, TCTTCTTTGGTGCCCGACA and CCAGCAGGAGATCCACCAAG for PBR. All primers were tested, and no primer-dimer was found in the Q-PCR reactions.

2.12. DNA synthesis assay

MDA-MB-231 cells were plated on 96-well plates in DMEM supplemented with 10% FBS containing 100 nM of siRNAs. After 72 h incubation, differences in DNA synthesis were analyzed by measuring the amount of 5-bromo-2′-deoxyuridine (BrdU) incorporation using the BrdU Cell Proliferation ELISA. Incorporation of BrdU was measured at 450 nm (reference at 690 nm) [45].

2.13. Lentiviral-mediated PBR RNA interference

Endogenously expressed siRNA effectors provide long-term silencing of the target gene and allow us to generate cell lines and transgenic organisms with a stable knockdown phenotype for functional studies. Double-promoter pFIV-H1/U6-copGFP™ siRNA Cloning and Expression Vector was used. pFIV siRNA Vectors are derived from feline immunodeficiency virus [46]. The pFIV Vectors are self-inactivating as a result of a deletion in the U3 region of 3′-ΔLTR. For each selected sequence, two complementary siRNA oligonucleotides (a sense strand and an anti-sense strand) were synthesized. In addition to the sense or anti-sense siRNA sequence the oligonucleotide included a 4-base sequence at the 5′ end of each oligonucleotide (AAAG on sense strand and AAAA on the anti-sense strand) to facilitate ligation with the vector. *E. coli* transformation and screening for siRNA template inserts for scrambled siRNA and PBR 548siRNA was performed following the manufacturer's protocol.

FIV pseudoviral particles containing a copy of PBR pFIV siRNA expression construct were then generated by mixing the following: 6 μl (3.0 μg) pFIV-PACK Packaging Plasmid Mix, 1.5 μg (3 μl) PBR pFIV expression construct, 400 μl DMEM medium without serum or antibiotics, and 20 μl Plus™ Reagent. The mixture was incubated at room temperature for 15 min and combined with Lipofectamine™ used to transfect 293T/17 cells at 50–70% confluency. DNA/Plus™/Lipofectamine™ complex was incubated with the cells for 5 h. The medium was then replaced with fresh DMEM medium, supplemented with 3% serum and antibiotics. The incubation continued for 48 h. Ten milliliters of the pseudovirus-containing medium was collected, centrifuged, and the supernatant containing the pseudoviral particles was used to infect MDA-MB-231 cells overnight. The virus supernatant was then

removed, and fresh DMEM with 10% FBS was added. Forty-eight hours later, cells were collected for FACS, cell counting and immunoblot analyses.

2.14. Cell proliferation assay

After subjecting cells to the above-described pFIV lentivirus protocol, cell proliferation was measured by direct cell counting using Coulter Counter Multisizer 3 after trypsinization.

2.15. Flow cytometry

A single cell suspension was prepared for cell cycle analysis as described previously [47]. In brief, MDA-MB-231 cells infected with PBR pFIV lentivirus, as described above, were trypsinized to obtain single cells, neutralized with medium containing serum, washed with 1× PBS and then resuspended in Citrate/DMSO buffer. Nuclei were isolated, the DNA was stained with propidium iodide and the nuclear DNA content was detected by flow cytometry [47]. The ModFit LT software (Verity Software House, Topsham, ME) was used to model the cell cycle data.

2.16. Immunoblots

After subjecting cells to the above-described pFIV lentivirus protocol, whole-cell extracts were prepared in lysis buffer (100 mM dithiothreitol, 2% sodium dodecyl sulfate, 50 mM Tris–HCl pH 6.8, 50% glycerol, 0.1% bromophenol blue). Equal amounts of protein were separated by SDS-PAGE in 4–20% Tris-Glycine Gels and electrotransferred onto a nitrocellulose membrane.

Proteins were visualized by enhanced chemiluminescence reaction and images were developed and analyzed using a Kodak Image Station 2000MM (New Haven, CT). The exposure time was adjusted so that no pixels in the image were saturated. Image-densitometric analysis of the immunoreactive protein bands was performed using the Kodak 1D software. The Region of Interest tool allowed us to define an area for analysis. The sum of the background-subtracted pixel values within the Region of Interest was used to compare the samples.

2.17. Statistics

Multiple means were compared using InStat's (GraphPad Inc.) one-way analysis of variance (ANOVA). p values for one-way ANOVAs are provided in the text. Comparisons between individual drug treatments and control treatments were made using an unpaired t-test. p values are provided in the text.

3. Results

3.1. PBR over-expression in non-aggressive MCF-7 human breast cancer cells

After stably transfecting human PBR cDNA and the pBi-EGFP bi-directional vector as described in the methods section, MOM and MIP cells were analyzed. While approximately 20 MOM stable transfectants were isolated, only 2 MIP stable transfectants (MIP1 and MIP2) could be isolated. EGFP expression was completely repressed by 1.0 μg/ml Dox in both MIP1 (Fig. 1A and B) and MIP2 cells (Fig. 1A), indicating that the Tet-Off system is fully functional in this cell line. EGFP fluorescence measurements indicated that EGFP expression was significantly repressed by serial Dox concentrations in MIP1 cells ($p < 0.001$ by ANOVA) and in MIP2 cells ($p < 0.001$), compared to untreated cells. Comparisons between individual Dox treatments and control were made using an unpaired t-test. Compared to MIP1 and MIP2 Dox-untreated controls, EGFP expression was significantly repressed by 10^{-4}, 10^{-2} or 10^{1} μg/ml Dox ($p < 0.001$ in both cell types).

3.2. Ligand binding to PBR in MCF-7 Tet-Off, MOM, MIP1 and MIP2 cells

As shown in Table 1, the MCF-7 Tet-Off cell line expressed approximately 10-fold fewer PBR ligand binding sites than the MDA-MB-231 cell line (B_{max} = 0.8 pmol/mg protein versus 8.7 pmol/mg protein, respectively). MOM cells also had a low capacity for PBR ligand binding (B_{max} of 0.5 pmol/mg protein, and was not statistically significant compared to MCF-7 Tet-Off cell line). MIP1 and MIP2 cells achieved maximal PBR ligand binding (B_{max}) of 4.9 and 2.1 pmol/mg protein, respectively. This increase in B_{max} was statistically significant for MIP1 ($p < 0.001$), but not for MIP2 cells, compared to MCF-7 Tet-Off cell line. In the presence of 1.0 μg/ml Dox, the B_{max} values for both MIP1 and MIP2 decreased to levels approximating those of MCF-7 Tet-Off and MOM cells (0.6 and 0.8 pmol/mg protein, respectively). K_d values, which represent reciprocals of ligand-binding affinities, were nearly identical (approximately 1.0 nM) for all cell lines under all conditions employed (Table 1). In preliminary experiments, we observed that PBR in MIP1 cells was mainly localized in the perinuclear/nuclear area (data not shown) as previously described in breast cancer cells [31].

Table 1 – PBR ligand binding characteristics of MCF-7 Tet-Off, MOM, and MIP cells

Cell line	K_d (nM)	B_{max} (pmol/mg protein)
MCF-7 Tet-Off	1.2 ± 0.23	0.8 ± 0.92
MOM	0.7 ± 0.16	0.5 ± 0.03
MIP1 − Dox	1.2 ± 0.20	4.9 ± 0.23***
MIP1 + Dox	0.9 ± 0.21	0.6 ± 0.04
MIP2 − Dox	1.3 ± 0.06	2.1 ± 0.03
MIP2 + Dox	1.2 ± 0.01	0.8 ± 0.03

Scatchard analyses of 40 μg of cell protein from MCF-7 Tet-Off, MOM, MIP1 and MIP2 cells were performed as described in Section 2. Scatchard analyses were also performed on MIP1 and MIP2 cells grown in the presence of 1.0 μg/ml Dox for 3 or more days. Data represents the mean ± S.E.M. of three independent experiments carried out in quadruplicate. Multiple B_{max} means were compared using one-way ANOVA, $p < 0.0001$. Comparisons between individual cell line's Bmax were made using an unpaired t-test. *** means compared to MCF-7 Tet-Off, $p < 0.001$.

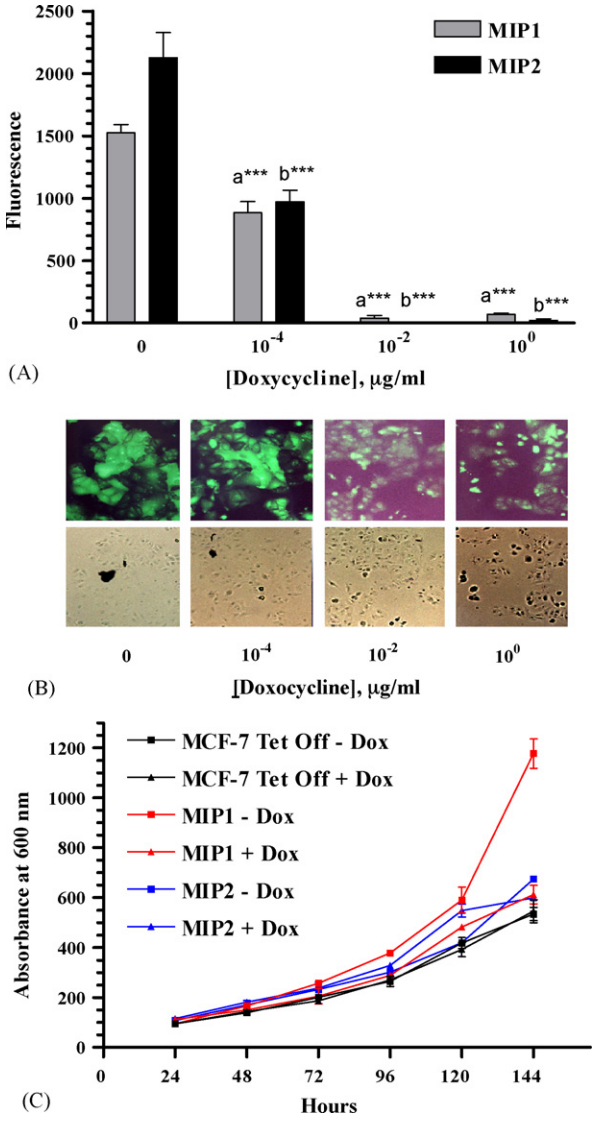

Fig. 1 – Repression of EGFP fluorescence by increasing doxycycline concentrations in MIP1 and MIP2 cells, and the effect of PBR transfection on the proliferation of MCF-7 Tet-Off cells. (A) MIP1 and MIP2 cells were seeded at a density of 5000 cells/well on a 96-well plate and grown for 4 days in medium containing 0.0, 0.0001, 0.1, or 1.0 μg/ml Dox. After 4 days, cells were washed in PBS and fluorescence was determined at 485 nm excitation, 510 nm emission. Data points represent the means ± S.E.M. of three independent experiments carried out in quadruplicate. a* $p < 0.001$ compared to MIP1 control and b*** $p < 0.001$ compared to MIP2 control. (B) MIP1 cells were layered on poly-D-lysine coated slides and grown under the same conditions as in (A). After 4 days, cells were fixed in 10% formaldehyde. The slides were then rinsed in distilled H_2O before mounting with Crystal/Mount. Phase-contrast images are beneath their corresponding fluorescent images. Each photograph was taken at 10× magnification. The higher background seen in the fluorescent images exposed to 0.01 and 1.0 μg/ml Dox was due to the low intensity of the signal. (C) Cell Proliferation Curves for MCF-7 Tet-Off, MIP1, and MIP2 Cells. Six-day growth curves were obtained for MCF-7 Tet-Off, MIP1, and MIP2 cells in the presence or absence of 1.0 μg/ml Dox. MIP1 cells proliferated at a much greater rate than MCF-7 Tet-Off cells in the absence of Dox ($p < 0.001$). Data represents the mean ± S.E.M. of three independent experiments carried out in eight replications.**

3.3. *Expression of vimentin in MIP1 and MIP2 cells*

Expression of the developmentally regulated intermediate filament protein vimentin is a marker of enhanced invasiveness and increased metastatic potential. Thus, it serves as an indicator of increased aggressive phenotype in breast cancer cells [48]. Immunocytochemical assays showing the expression of vimentin in the MCF-7 Tet-Off, MDA-MB-231, MIP1, and MIP2 cells were performed (data not shown). As MCF-7 cells are vimentin-negative and as MDA-MB-231 cells are vimentin-positive [48], MDA-MB-231 cells were used as a positive control in these experiments. Vimentin immunostaining was found in MCF-7 Tet-Off, MIP1 and MIP2 cell lines, and strong immunostaining occurred in MDA-MB-231 cells (Fig. 2). However, there were no gross differences in vimentin expression among MCF-7 Tet-Off, MIP1 and MIP2 cell lines.

3.4. *Effects of PBR transfection on the proliferation of MCF-7 Tet-Off cells*

Further functional studies were performed to examine whether increased PBR expression may lead to increased cell proliferation, as our previous studies had indicated [31,39,40]. Indeed, in the presence of 10% FBS, MIP1 cells proliferated at a much greater rate than MCF-7 Tet-Off cells in the absence of Dox ($p < 0.001$; Fig. 1C). This effect was abrogated by the addition of 1.0 μg/ml Dox. No differences were seen between the proliferation rates of MIP2 and MCF-7 Tet-Off cells in the absence of Dox. Preliminary studies did not show any significant difference between the MCF-7 Tet-Off and the original MCF-7 cell line (data not shown). In additional experiments, proliferation of MOM cells did not differ from that of MCF-7 Tet-Off cells. Neither the MIP1 nor the MIP2 cell line displayed a greater ability to grow in soft agar than the MCF-7 Tet-Off parental cell line (data not shown).

3.5. *siRNAs targeting PBR down-regulate PBR mRNA in MDA-MB-231 breast cancer cells*

Seventy-two hours treatment of cells with siRNAs (100 nM) targeting various PBR coding regions decreased PBR mRNA expression by about 50% (Fig. 3A). Multiple PBR mRNA means were compared by ANOVA among all the groups, showing that 361, 537, 548 PBR siRNAs significantly decreased PBR mRNA levels ($p < 0.0001$, ANOVA). 548 PBR siRNA was used in the following functional studies.

3.6. *siRNAs targeting PBR down-regulate radioligand binding in MDA-MB-231 breast cancer cells*

The inhibition of PBR mRNA expression in MDA-MB-231 cells after 100 nM PBR-specific 548 siRNAs treatment for 72 h resulted in a statistically significant ($p < 0.001$) inhibition of ligand binding to PBR compared to control (Fig. 3B).

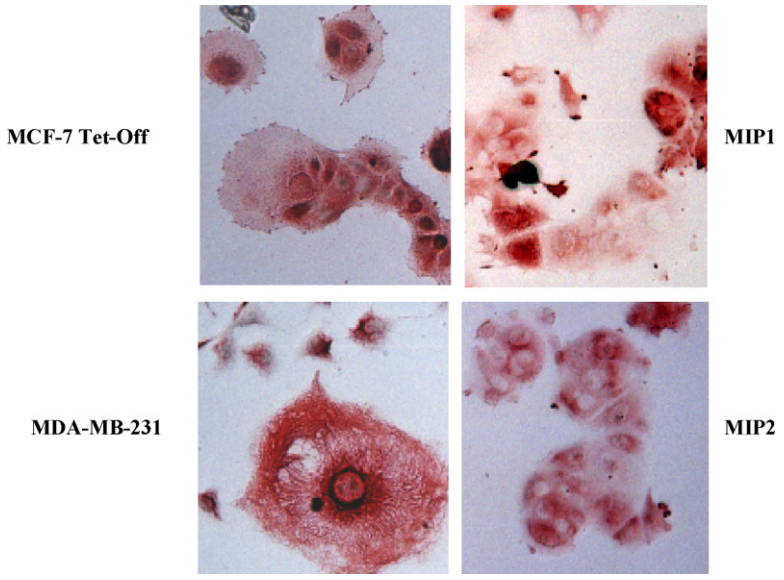

Fig. 2 – Vimentin immunocytochemistry. 20,000 cells per well for MCF-7 Tet-Off, MIP1, and MIP2 cells and 5000 cells per well for MDA-MB-231 cells were loaded onto poly-D-lysine coated 8-well slides and incubated for 48 h. Cells were fixed and vimentin immunostaining was carried out as described in Section 2. Phase-contrast images were taken at 10× magnification.

3.7. *Silencing PBR expression inhibits the BrdU incorporation of MDA-MB-231 cells*

Following treatment of MDA-MB-231 cells with 100 nM PBR-specific 548 siRNAs for 72 h, the amount of BrdU incorporation also decreased in a manner parallel to the decrease in PBR mRNA expression (Fig. 3C; $p < 0.0001$, ANOVA).

3.8. *Effect of silencing PBR expression on cell proliferation and cell cycle*

After its integration into MDA-MB-231, the pFIV effector cassette continuously and stably produced high levels of siRNA molecules in the target cells. The pFIV-H1/U6-copGFP™ contains a copGFP reporter gene, which is similar to EGFP but

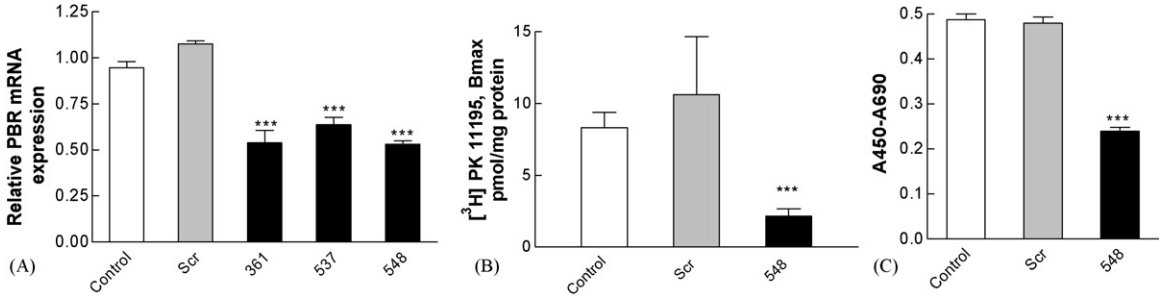

Fig. 3 – siRNAs targeting PBR decrease PBR mRNA and proliferation in MDA-MB-231 breast cancer cells. (A) MDA-MB-231 cells were either mock-transfected or transfected with 100 nM siRNAs targeting different coding region of PBR or scrambled siRNA, and analyzed 72 h later for PBR mRNA expression by Q-PCR. Results shown are means ± S.E.M. from three independent experiments ($n = 9$). Multiple PBR mRNA means were compared by ANOVA among all the groups, showing that PBR siRNA significantly decreased PBR mRNA levels ($p < 0.0001$, ANOVA). (B) MDA-MB-231 cells were either mock-transfected or transfected with 100 nM 548 siRNA targeting a PBR coding region or scrambled siRNA. Cells were analyzed 72 h later for PBR expression using a [^{3}H]PK 11195 ligand binding assay. The inhibition of PBR mRNA expression in MDA-MB-231 cells after 100 nM PBR-specific 548 siRNAs treatment for 72 h resulted in a statistically significant ($p < 0.001$) inhibition of ligand binding to PBR compared to control. Results shown are means ± S.E.M. from two independent experiments ($n = 6$). (C) After either mock-transfected or transfected with 100 nM PBR-548 siRNA or scrambled siRNA for 72 h, the amount of BrdU incorporation was determined in MDA-MB-231 as described in Section 2. Results shown are means ± S.E.M. from three independent experiments ($n = 9$). The amount of BrdU incorporation decreased in a manner parallel to the decrease in PBR mRNA expression in 548 siRNA treated cells ($p < 0.0001$, ANOVA).

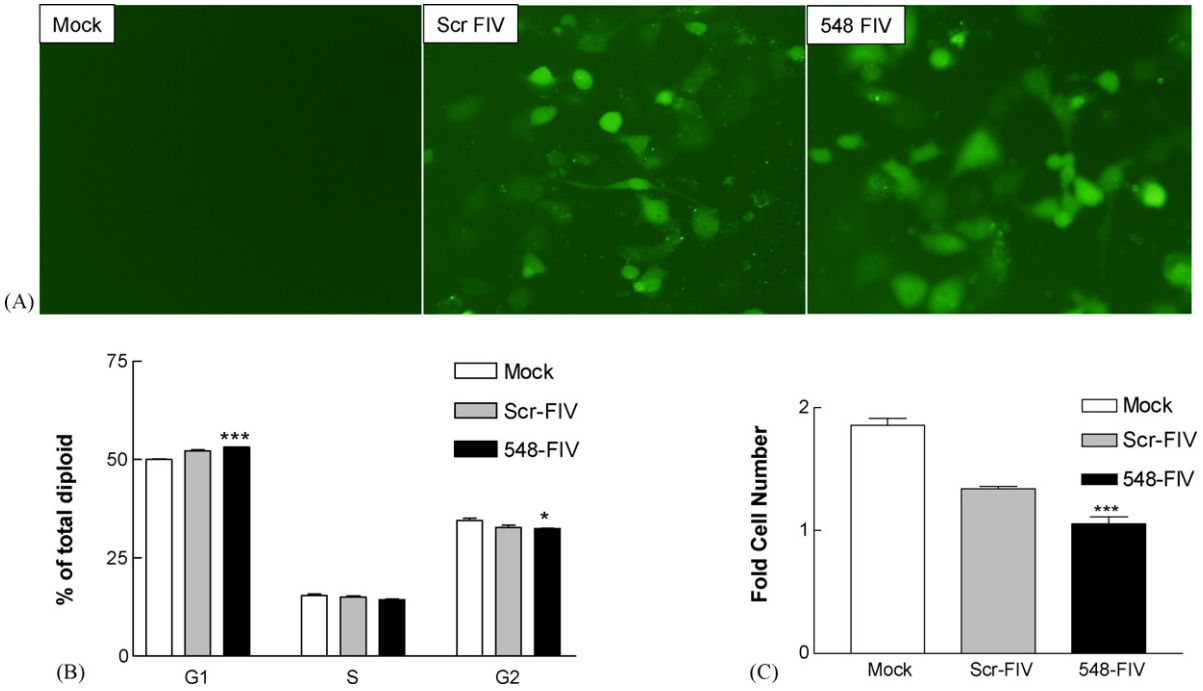

Fig. 4 – Effect of silencing PBR expression on cell proliferation and cell cycle. (A) After its integration into MDA-MB-231, the pFIV effector cassette continuously and stably produced high levels of siRNA molecules in target cells. MDA-MB-231 cells were either transfected with 548 FIV siRNA targeting coding region of PBR or scrambled FIV siRNA, and analyzed 72 h later by flow cytometry to define the effect of the PBR siRNA treatment on cell cycle (B) and cell proliferation (C). Compared to Mock or scrambled FIV siRNA, 548 FIV PBR siRNAs increased the percent of cell in G1-phase significantly ($p < 0.0001$), whereas there was a small decrease in the percentage of cells in S (not statistically significant) and G2 phases ($p < 0.05$). 548 FIV MDA-MB-231 cells proliferated at a much lower rate than control and scrambled FIV siRNA ($p < 0.0001$, ANOVA). Results shown are means ± S.E.M. from four independent experiments.

has a brighter color (Fig. 4A). Target cells that stably express the effector molecule can be isolated using the selection contained in the expression vector construct (e.g. GFP). MDA-MB-231 cells were either transfected with 548 FIV siRNA targeting coding region of PBR or scrambled FIV siRNA, and analyzed 72 h later by flow cytometry to define the effect of the PBR siRNA treatment on cell cycle (Fig. 4B) and cell proliferation (Fig. 4C). Compared to Mock or scrambled FIV siRNA, 548 FIV PBR siRNAs increased the percent of cell in G1-phase significantly ($p < 0.0001$), whereas there was a small decrease in the percentage of cells in S (not statistically significant) and G2 phases ($p < 0.05$). 548 FIV MDA-MB-231 cells proliferated at a much lower rate than control and scrambled FIV siRNA ($p < 0.0001$, ANOVA). When tissue culture supernatants were colleted and cells were counted, cell numbers in the supernatants was very low compared to the cells attached to the plate. Moreover, there was no significant difference between cell numbers measured in the supernatants from different treatments (data not shown).

3.9. *Effect of silencing PBR expression on CDKIs, cyclins, caspase-3, PCNA, phospho-p53 (p-p53), and Rb protein*

To elucidate the mechanism underlying the translation of changes in PBR levels into changes in cell cycle and proliferation, we examined the expression of key proteins involved in regulating these processes. Inhibition of PBR protein expression by treatment of MDA-MB-231 cells with PBR 548 FIV was correlated with significant increases in cyclin A, $p21^{WAF1/CIP1}$, cleaved caspase-3 ($p < 0.05$, ANOVA), and p-p53 (Ser15) ($p < 0.01$, ANOVA). The changes were also seen in the expression levels of cyclin B, PCNA, Rb protein expression (not statistically significant) (Fig. 5). However, these changes were not consistent across experiments.

4. Discussion

The results presented here provide convincing evidence that PBR is involved in regulating cell cycle and proliferation in breast cancer cells. PBR could play a role in mediating the increased cell proliferation that occurs in breast cancer and in certain other forms of cancer.

We found that stable transfection of the MCF-7 Tet-Off derivative of MCF-7 cells with the full-length human PBR cDNA resulted in MIP1 and MIP2 cells that exhibited an increase in PBR ligand binding. Growth assays showed that MIP1 cells grew at a greater rate than MCF-7 Tet-Off cells. The finding that Dox abolished this difference in growth rate strongly indicates that the increased cell proliferation were a *direct* result of increased PBR expression and not a by-product of transfection. Further, the lack of differences in cell proliferation between MCF-7

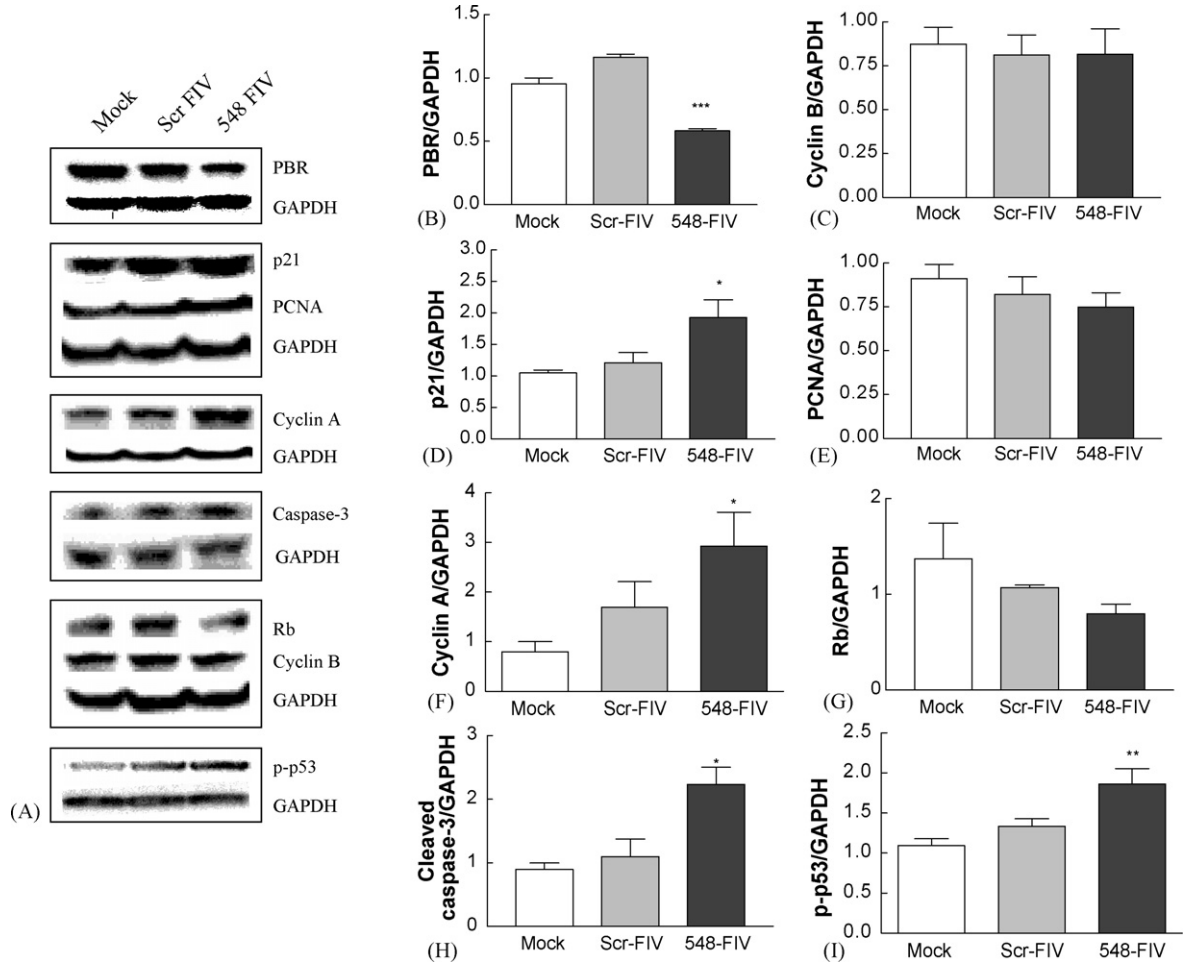

Fig. 5 – Effect of silencing PBR expression on CDKIs, cyclins, caspase-3, PCNA, p-p53 (Ser15), and Rb protein levels. MDA-MB-231 cells were either mock-transduced or transduced with packaged pFIV expression construct virus targeting coding region of PBR or scrambled siRNA. Cells were analyzed 3 days later for PBR protein expression by Western blot analysis (A) followed by image-densitometric analysis of the immunoreactive protein bands (B–I). Inhibition of PBR protein expression (B) by treatment of MDA-MB-231 cells with PBR 548 FIV was correlated with increases in $p21^{WAF1/CIP1}$ (D), cyclin A (F), cleaved caspase-3 (H) ($p < 0.05$, ANOVA), and p-p53 (Ser15) (I) ($p < 0.01$, ANOVA). Changes of cyclin B (C), PCNA (E), and Rb (G) protein expression were also observed but they were not consistent across experiments (not statistically significant). Equal loading was assessed using anti-GAPDH. Blots shown are representative of one experiment. Similar results were obtained in three other independent experiments. Bar graphs show means ± S.E.M. generated from image-densitometric analysis of the immunoreactive protein bands from three or four independent experiments.

Tet-Off and MIP2 cells, which bind the PBR ligand less than MIP1 cells, indicates that a certain threshold level of PBR expression must be surpassed in order for increased cell proliferation to occur.

The finding that increasing the expression of PBR in MIP1 cells can enhance cell proliferation supports other findings that PBR could be correlated with malignancy. PBR site densities are as much as 12-fold higher in high-grade astrocytomas and glioblastomas than in normal brain tissue [15]. PBR is highly up-regulated in high-grade human astrocytomas relative to low grade tumors [16]. Additionally, binding of the PBR-specific ligand, PK11195 is two-fold greater in glioblastomas than in normal human gray matter [28]. The relatively high PBR binding density was associated with enhanced tumorigenicity and cell proliferation rate in glioma cells, and PBR was functionally involved in apoptosis in glioma cells [49].

Other recent results have indicated that the expression of PBR is correlated with carcinogenic potential. PBR binding occurs to a much greater extent in aggressive, estrogen receptor (ER)-negative MDA-MB-231 cells than in non-aggressive, ER-positive MCF-7 cells [31]. Beinlich and colleagues [50] have indicated that specific high-affinity binding of a PBR agonist ([^{3}H]Ro5-4864) to PBR occurred with highest capacity in the ER-negative, progesterone receptor (PR)-negative BT-20 and MDA-MB-435-5 breast cancer cell lines but with only low capacity in ER-positive, PR-positive MCF-7, T47-D and BT-474 breast cancer cell lines.

PBR protein expression and ligand binding are up-regulated in aggressive metastatic human breast tumor biopsies [31] by a

mechanism(s) that may related to PBR gene amplification [39,40]. This suggests that PBR may play an important role in the proliferation of human breast tumors.

Taken together, the data presented here provide crucial support of the view that PBR directly influences the regulation of cell proliferation in cancer cells. Using vimentin immunostaining as a marker of the aggressive phenotype of the cells, we found no gross differences in vimentin expression among MCF-7 Tet-Off, MIP1 and MIP2 cell lines. Although the use of vimentin alone may be limiting, these data suggest that although the amount of PBR protein per cell may serve as the index of carcinogenesis, the level of PBR expression does not appear to account for other phenotypic differences that exist between non-aggressive and aggressive human breast cancer cells. Additionally, PBR transfection did not affect the ability of MCF-7 Tet-Off cells to grow in soft agar (anchorage-independent cell growth; the hallmark of uncontrolled tumorigenic proliferation) (data not shown).

In the present study, PBR–siRNA duplexes were used to evaluate the role of PBR in cell proliferation in aggressive, PBR-enriched, MDA-MB-231 human breast cancer cells. The goal of this work was to determine the contribution of PBR to invasiveness and metastatic potential, which are important phenotypic characteristics of breast cancer cell lines. Our finding that inhibition of PBR mRNA expression by PBR–siRNAs led to reduced proliferation of MDA-MB-231 cells agrees with our previous results that *in vitro* treatment of these cells or treatment of nude mice bearing xenografts of these cells with the standardized leaf extract of *Ginkgo biloba* (EGb 761) and ginkgolide B inhibited PBR gene expression and cell proliferation [44,45].

Earlier studies by Sanger et al. [51] demonstrated that a strong correlation exists between increased expression of PBR ligand binding and the increase in the percentage of cells in the S phase, which suggests that PBR regulates cell proliferation by influencing cell cycle function. Further studies showed that low concentrations of PBR ligands stimulated proliferation of the aggressive BT-20 breast cancer cell line [50], whereas high micromolar concentrations inhibited proliferation. Thus, nanomolar concentrations of PBR ligands may enhance the entry of these cells into the S phase of the cell cycle, whereas high micromolar concentrations may lead to an accumulation of cells in the G0/G1 phase [51]. Carmel and colleagues [52] also found that high micromolar concentrations of PBR ligands also inhibit proliferation of non-aggressive MCF-7 cells by inducing the cells to accumulate in the G0/G1 phase. These studies [51,52] provide persuasive evidence that PBR influences cell proliferation by regulating cell cycle staging.

The use of PBR ligands induced hepatocellular carcinoma cells to arrest at both the G1/S- and G2/M-checkpoints [53]. We report here that inhibition of PBR mRNA expression by PBR–siRNAs led to cell cycle arrest at G2 phase. These data also suggest that the PBR protein itself may be linked to signaling pathways involved in the regulation of cell cycle. We examined this hypothesis by looking at the expression levels of molecules involved in cell cycle control.

Endogenously expressed siRNA effectors provide long-term silencing of the target gene and allow us to generate cell lines and transgenic organisms with a stable knockdown phenotype for functional studies. Lentiviral expression vectors are the most effective vehicles for delivering genetic material to almost any mammalian cell-including non-dividing cells and whole model organisms [54]. Using lentiviral-mediated PBR RNAi, we observed that inhibition of PBR expression is linked to significant increases in $p21^{WAF1/CIP1}$, p-p53 and cleaved caspase-3 protein expression, as well as a consistent increase in cyclin A protein expression. Decreased cyclin B, PCNA and Rb protein expression levels were also observed, although not in a consistent manner. $p21^{WAF1/CIP1}$ was initially identified as an inhibitor of cyclin-dependent protein kinase (Cdk) activity, and was shown to inhibit each member of the Cdk family of proteins that is involved in cell cycle control [55,56]. Related studies have revealed that $p21^{WAF1/CIP1}$ is a downstream mediator of the p53 tumor-suppressor and that $p21^{WAF1/CIP1}$ may play a prominent role in inducing apoptosis and cell cycle arrest [55,57–61].

p53 is a transcription factor present at minute levels in any normal cells. Upon various types of stress (DNA damage, hypoxia, nucleotide pool depletion, viral infection, oncogene activation), posttranslational modifications lead to p53 stabilization and activation. Although the number of genes activated by p53 is rather large, the outcome of p53 activation is cell cycle arrest in G1 or G2, or apoptosis [62,63]. The cell growth arrest by p53 activates of the DNA repair system of the cell [63]. Thus, our finding that inhibition of PBR expression is associated with increased expression of $p21^{WAF1/CIP1}$ and p-p53 is of interest, particularly because it links PBR inhibition via $p21^{WAF1/CIP1}$ up-regulation to mechanisms involved in apoptosis and tumor suppression.

Many studies have shown that various anticancer drugs enhance the expression of $p21^{WAF1/CIP1}$ [64–66]. Increased expression of $p21^{WAF1/CIP1}$ in anaplastic thyroid cancer cells (KAT-4 cells) enhanced the antineoplastic activity of paclitaxel and its capacity to induce apoptosis [67]. Additionally, transcription of $p21^{WAF1/CIP1}$ was increased in human breast cancer cell lines MCF-7 and MDA-MB-468 by treatment with the DNA topoisomerase I inhibitors 10-hydroxycamptothecin and camptothecin, both of which have been shown to have therapeutic effects in various models of human breast cancer [68]. Phenylacetate, a member of a new class of antineoplastic drugs, arrested growth of MCF-7 cells associated with overexpression of $p21^{WAF1/CIP1}$ [69]. In agreement with these findings, we observed a significant inhibitory effect of PBR–siRNA treatment on cell proliferation.

Caspase-3 is one of the key executioners of apoptosis, as it is either partially or totally responsible for the proteolytic cleavage of many key proteins [70]. Activation of caspase-3 requires proteolytic processing of its inactive zymogen into activated p17 and p12 fragments.

Progression of the mammalian cell cycle is regulated by phosphorylation of many key proteins, such as cyclins. Several classes of cyclins act as regulatory subunits for Cdks. These cyclin-Cdk holoenzymes are essential for proper control of cell cycle progression because they regulate a variety of substrates whose activity is required for cell cycle transitions. We report here that in cells with reduced PBR levels, there was a significant increase in cyclin A, but no significant changes in cyclin B or PCNA protein levels. Cyclin A seems to be required for both S and G2 phases [71]. The retinoblastoma (Rb) tumor suppressor

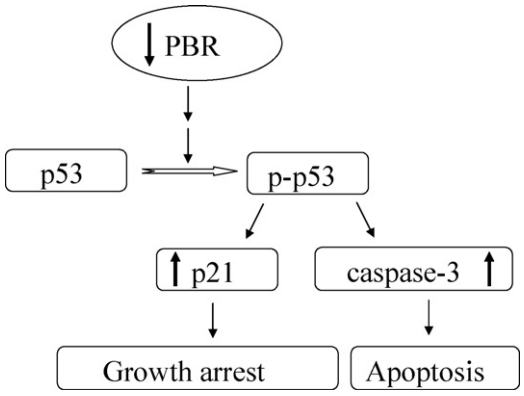

Fig. 6 – Schematic representation of the PBR-mediated regulation of cell growth in MDA-MB-231 human breast cancer cells. The data presented suggest that reduction of PBR levels results in the activation of p53 (phopshorylation at Ser15), induction of the cyclin-dependent kinase inhibitor $p21^{WAF1/CIP1}$ and cleaved caspase-3 levels leading to growth arrest and apoptosis.

gene product levels were reduced, although not in a significant manner, in cells where PBR levels were knocked down. The lack of effect of PBR–siRNA treatment of MDA-MB-231 cells on cyclin B, and PCNA may be indicating that inhibition of PBR expression has some degree of selectivity.

There is a great deal more to learn about PBR and its role in cell proliferation. The present studies indicate that there is a link between PBR expression levels, p53 activation, and rate of cell proliferation in human breast cancer cells (Fig. 6). It seems likely that PBR has the versatility required to perform many different cellular functions while maintaining its identity as the major site involved in mediating the incorporation of cholesterol into cellular membranes. Indeed, we recently demonstrated that the *Arabidopsis thaliana* PBR homologue retains the ability to transport cholesterol [72]. We envision that the development of methods based on regulating tumor cell proliferation by PBR manipulation opens up many new avenues for developing anticancer therapies. In showing that PBR–siRNAs can inhibit the proliferation of human breast cancer cells, the results provided herein represent a first step toward achieving this goal. Given that PBR expression is increased in human colonic, brain, ovarian, and breast cancer biopsies [15,24,26,27], it seems that manipulation of PBR by treatment with PBR–siRNAs could be useful in treating a broad variety of cancers.

Acknowledgements

This work was supported by a grant from the Department of Defense (DAMD17-99-1-9200). We thank the Tissue Culture Core facility of the Lombardi Comprehensive Cancer Center for assistance in this project. We also thank Dr. F. DeFeudis (Institute for Biosciences, Westboro, MA) for critically reviewing the manuscript.

REFERENCES

[1] Lippman ME. The development of biological therapies for breast cancer. Science 1993;259:631–2.
[2] Papadopoulos V. Peripheral-type benzodiazepine/diazepam binding inhibitor receptor: biological role in steroidogenic cell function. Endocr Rev 1993;14:222–40.
[3] Gavish M, Bachman I, Shoukrun R, Katz Y, Veenman L, Weisinger G, et al. Enigma of the peripheral benzodiazepine receptor. Pharmacol Rev 1999;51:629–50.
[4] Lacapère JJ, Delavoie F, Li H, Peranzi G, Maccario J, Papadopoulos V, et al. Structural and functional study of reconstituted peripheral benzodiazepine receptor (PBR). Biochem Biophys Res Commun 2001;284:536–641.
[5] Li H, Yao Z, Degenhardt B, Teper G, Papadopoulos V. Cholesterol binding at the cholesterol recognition/interaction amino acid consensus (CRAC) of the peripheral-type benzodiazepine receptor and inhibition of steroidogenesis by an HIV TAT-CRAC peptide. Proc Natl Acad Sci USA 2001;98:1267–72.
[6] Hirsch JD, Beyer CF, Malkowitz L, Beer B, Blume AJ. Mitochondrial benzodiazepine receptors mediate inhibition of mitochondrial respiratory control. Mol Pharmacol 1989;35:157–63.
[7] Papadopoulos V, Dharmarajan AM, Li H, Culty M, Lemay M, Sridaran R. Mitochondrial peripheral-type benzodiazepine receptor expression: correlation with the GnRH-agonist induced apoptosis in the corpus luteum. Biochem Pharmacol 1999;58:1389–93.
[8] Carayon P, Portier M, Dussossoy D, Bord A, Petitpretre G, Canat X, et al. Involvement of peripheral benzodiazepine receptors in the protection of hematopoietic cells against oxygen radical damage. Blood 1996;87:3170–8.
[9] Rey C, Mauduit C, Naureils O, Benahmed M, Lousiot P, Gasnier F. Up-regulation of mitochondrial peripheral benzodiazepine receptor expression by tumor necrosis factor alpha in testicular Leydig cells. Possible involvement in cell survival. Biochem Pharmacol 2000;60:1639–46.
[10] Hardwick M, Rone J, Han J, Haddad B, Papadopoulos V. Peripheral-type benzodiazepine receptor levels correlate with the ability of human breast cancer MDA-MB-231 cell line ability to grow in SCID mice. Int J Cancer 2001;94:322–7.
[11] Hauet T, Han Z, Wang Y, Hameury F, Jayle C, Gibelin H, et al. Modulation of peripheral-type benzodiazepine receptor levels in a perfusion injury pig kidney-graft model. Transplantation 2002;74:1507–15.
[12] Morin D, Papadopoulos V, Tillement J-P. Prevention of cell damage in ischemia: novel molecular targets in mitochondria. Expert Opin Therap Target 2002;6:315–34.
[13] Castedo M, Perfettini JL, Kroemer G. Mitochondrial apoptosis and the peripheral benzodiazepine receptor: a novel target for viral and pharmacological manipulation. J Exp Med 2002;96:1127–39.
[14] Garnier M, Dimchev AB, Boujrad N, Price JM, Musto NA, Papadopoulos V. In vitro reconstitution of a functional peripheral-type benzodiazepine receptor from mouse Leydig tumor cells. Mol Pharmacol 1994;45:201–11.
[15] Cornu P, Benavides J, Scatton B, Hauw JJ, Philippon J. Increase in omega 3 (peripheral-type benzodiazepine) binding site densities in different types of human brain tumors. A quantitative autoradiography study. Acta Neurochir 1992;119:146–52.
[16] Miettinen H, Kononen J, Haapasalo H, Helen P, Sallinen P, Harjuntausta T, et al. Expression of peripheral-type benzodiazepine receptor and diazepam binding inhibitor in human astrocytomas: relationship to cell proliferation. Cancer Res 1995;55:2691–5.

[17] Ikezaki K, Black KL. Stimulation of cell growth and DNA synthesis by peripheral benzodiazepine. Cancer Lett 1990;49:115–20.
[18] Bruce JH, Ramirez AM, Lin L, Oracion A, Agarwal RP, Norenberg MD. Peripheral-type benzodiazepines inhibit proliferation of astrocytes in culture. Brain Res 1991;564:167–70.
[19] Neary JT, Jorgensen SL, Oracion AM, Bruce JH, Norenberg MD. Inhibition of growth factor-induced DNA synthesis in astrocytes by ligands of peripheral-type benzodiazepine receptors. Brain Res 1996;675:27–30.
[20] Clarke GD, Ryan PJ. Tranquillizers can block mitogenesis in 3T3 cells and induce differentiation in Friend cells. Nature 1980;287:160–1.
[21] Laird 2nd HE, Gerrish KE, Duerson KC, Putnam CW, Haddock-Russell D. Peripheral benzodiazepine binding sites in Nb 2 node lymphoma cells: effects on prolactin-stimulated proliferation and ornithine decarboxylase activity. Eur J Pharm 1989;171:25–35.
[22] Chelli B, Lena A, Vanacore R, Pozzo ED, Costa B, Rossi L, et al. Peripheral benzodiazepine receptor ligands: mitochondrial transmembrane potential depolarization and apoptosis induction in rat C6 glioma cells. Biochem Pharmacol 2004;68:125–34.
[23] Maaser K, Grabowski P, Oezdem Y, Krahn A, Heine B, Stein H, et al. Up-regulation of the peripheral benzodiazepine receptor during human colorectal carcinogenesis and tumor spread. Clin Cancer Res 2005;11:1751–6.
[24] Katz Y, Eitan A, Amiri Z, Gavish M. Dramatic increase in peripheral benzodiazepine binding sites in human colonic carcinoma as compared to normal colon. Eur J Pharmacol 1988;148:483–4.
[25] Katz Y, Eitan A, Gavish M. Increase in peripheral benzodiazepine binding sites in colonic adenocarcinoma. Oncology 1990;47:139–42.
[26] Katz Y, Ben-Baruch G, Kloog Y, Menczer J, Gavish M. Increased density of peripheral benzodiazepine-binding sites in ovarian carcinomas as compared with benign ovarian tumours and normal ovaries. Clin Sci (London) 1990;78:155–8.
[27] Han Z, Slack RS, Li W, Papadopoulos V. Expression of peripheral benzodiazepine receptor (PBR) in human tumors: relationship to breast, colon and prostate tumor progression. J Rec Res Sign Transd 2003;23:225–38.
[28] Pappata S, Cornu P, Samson Y, Prenant C, Benavides J, Scatton B, et al. PET study of carbon-11-PK 11195 binding to peripheral-type benzodiazepine sites in glioblastoma: a case report. J Nuclear Med 1991;32:1608–10.
[29] Ratcliffe SL, Matthews EK. Modification of the photodynamic action of delta-aminolaevulinic acid (ALA) on rat pancreatoma cells by mitochondrial benzodiazepine receptor ligands. Br J Cancer 1995;71:300–5.
[30] Kupczyk-Subotkowska L, Siahaan TJ, Basile AS, Friedman HS, Higgins PE, Song D, et al. Modulation of mephalan resistance in glioma cells with a peripheral benzodiazepine receptor ligand-mephalan conjugate. J Med Chem 1997;40:1726–30.
[31] Hardwick M, Fertikh D, Culty M, Li H, Vidic B, Papadopoulos V. Peripheral-type benzodiazepine receptor (PBR) in human breast cancer: correlation of breast cancer cell aggressive phenotype with PBR expression, nuclear localization, and PBR-mediated cell proliferation and nuclear transport of cholesterol. Cancer Res 1999;59:831–42.
[32] Maaser K, Hopfner M, Jansen A, Weisinger G, Gavish M, Kozikowski AP, et al. Specific ligands of the peripheral benzodiazepine receptor induce apoptosis and cell cycle arrest in human colorectal cancer cells. Br J Cancer 2001;85:1771–80.
[33] Sutter AP, Maaser K, Hopfner M, Barthel B, Grabowski P, Faiss S, et al. Specific ligands of the peripheral benzodiazepine receptor induce apoptosis and cell cycle arrest in human esophageal cancer cells. Int J Cancer 2002;102:318–27.
[34] Camins A, Diez-Fernandez C, Pujadas E, Camarasa J, Escubedo E. A new aspect of the antiproliferative action of peripheral-type benzodiazepine receptor ligands. Eur J Pharmacol 1995;272:289–92.
[35] Maaser K, Sutter AP, Krahn A, Hopfner M, Grabowski P, Scherubl H. Cell cycle-related signaling pathways modulated by peripheral benzodiazepine receptor ligands in colorectal cancer cells. Biochem Biophys Res Commun 2004;324:878–86.
[36] Maaser K, Sutter AP, Scherubl H. Mechanisms of mitochondrial apoptosis induced by peripheral benzodiazepine receptor ligands in human colorectal cancer cells. Biochem Biophys Res Commun 2005;332:646–52.
[37] Decaudin D, Castedo M, Nemati F, Beurdeley-Thomas A, De Pinieux G, Caron A, et al. Peripheral benzodiazepine receptor ligands reverse apoptosis resistance of cancer cells in vitro and in vivo. Cancer Res 2002;62:1388–93.
[38] Decaudin D. Peripheral benzodiazepine receptor and its clinical targeting. Anticancer Drugs 2004;15:737–45.
[39] Hardwick M, Rone J, Han J, Haddad B, Papadopoulos V. Peripheral-type benzodiazepine receptor levels correlate with the ability of human breast cancer MDA-MB-231 cell line ability to grow in SCID mice. Int J Cancer 2001;94:322–7.
[40] Hardwick M, Rone J, Barlow K, Haddad B, Papadopoulos V. Peripheral-type benzodiazepine receptor (PBR) gene amplification in MDA-MB-231 aggressive breast cancer cells. Cancer Genet Cytogen 2002;139:48–51.
[41] Galiegue S, Casellas P, Kramar A, Tinel N, Simony-Lafontaine J. Immunohistochemical assessment of the peripheral benzodiazepine receptor in breast cancer and its relationship with survival. Clin Cancer Res 2004;10:2058–64.
[42] Bradford MM. A rapid and sensitive method for the quantification of microgram quantities of protein using the principle of protein-dye binding. Anal Biochem 1976;72:248–54.
[43] Kletsas D, Li W, Han Z, Papadopoulos V. Peripheral-type benzodiazepine receptor (PBR) and PBR drug ligands in fibroblast and fibrosarcoma cell proliferation: role of ERK, c-jun and ligand-activated PBR-independent pathways. Biochem Pharm 2004;67:1927–32.
[44] Li W, Pretner E, Shen L, Drieu K, Papadopoulos V. Common gene targets of Ginkgo biloba extract (EGb 761) in human tumor cells:relation to cell growth. Cell Mol Biol (Noisy-le-grand) 2002;48:655–62.
[45] Papadopoulos V, Kapsis A, Li H, Amri H, Hardwick M, Culty M, et al. Drug-induced inhibition of the peripheral-type benzodiazepine receptor expression and cell proliferation in human breast cancer cells. Anticancer Res 2000;20:2835–48.
[46] Poeschla EM, Wong-Staal F, Looney DJ. Efficient transduction of nondividing human cells by feline immunodeficiency virus lentiviral vectors. Nat Med 1998;4:354–7.
[47] Vindelov LL, Christensen IJ, Nissen NI. A detergent-trypsin method for the preparation of nuclei for flow cytometric DNA analysis. Cytometry 1983;3:323–7.
[48] Thompson EW, Paik S, Brunner N, Sommers CL, Zugmaier G, Clarke R, et al. Association of increased basement membrane invasiveness with absence of estrogen receptor and expression of vimentin in human breast cancer cell lines. J Cell Physiol 1992;150:534–44.
[49] Veenman L, Levin E, Weisinger G, Leschiner S, Spanier I, Snyder SH, et al. Peripheral-type benzodiazepine receptor

density and in vitro tumorigenicity of glioma cell lines. Biochem Pharmacol 2004;68:689–98.
[50] Beinlich A, Strohmeier R, Kaufmann M, Kuhl H. Specific binding of benzodiazepines to human breast cancer cell lines. Life Sci 1999;65:2099–108.
[51] Sanger N, Strohmeier R, Kaufmann M, Kuhl H. Cell cycle-related expression and ligand binding of peripheral benzodiazepine receptor in human breast cancer cell lines. Eur J Cancer 2000;36:2157–63.
[52] Carmel I, Fares FA, Leschiner S, Scherubl H, Weisinger G, Gavish M. Peripheral-type benzodiazepine receptors in the regulation of proliferation of MCF-7 human breast carcinoma cell line. Biochem Pharmacol 1999;58:273–8.
[53] Sutter AP, Maaser K, Grabowski P, Bradacs G, Vormbrock K, Hopfner M, et al. Peripheral benzodiazepine receptor ligands induce apoptosis and cell cycle arrest in human hepatocellular carcinoma cells and enhance chemosensitivity to paclitaxel, docetaxel, doxorubicin and the Bcl-2 inhibitor HA14-1. J Hepatol 2004;41:799–807.
[54] Haddrick M, Han-Liu Z, Lau A, Heaphy S, Cann AJ. Production of non-infectious human immunodeficiency virus-like particles which package specifically viral RNA. J Virol Meth 1996;61:89–93.
[55] Zhang H, Hannon GJ, Beach D. p21-containing cyclin kinases exist in both active and inactive states. Genes Dev 1994;15:1750–8.
[56] Dulic V, Stein GH, Far DF, Reed SI. Nuclear accumulation of p21Cip1 at the onset of mitosis: a role at the G2/M-phase transition. Mol Cell Biol 1998;18:546–57.
[57] el-Deiry WS, Tokino T, Velculescu VE, Levy DB, Parsons R, Trent JM, et al. WAF1, a potential mediator of p53 tumor suppression. Cell 1993;75:817–25.
[58] Sheikh MS, Rochefort H, Garcia M. Overexpression of p21WAF1/CIP1 induces growth arrest, giant cell formation and apoptosis in human breast carcinoma cell lines. Oncogene 1995;11:1899–905.
[59] Strasser A. Dr. Josef Steiner Cancer Research Prize Lecture: the role of physiological cell death in neoplastic transformation and in anti-cancer therapy. Int J Cancer 1999;81:505–11.
[60] Gómez-Navarro J, Arafat W, Xiang J. Gene therapy for carcinoma of the breast: pro-apoptotic gene therapy. Breast Cancer Res 1999;2:32–44.
[61] Kim JS, Baek SJ, Bottone Jr FG, Sali T, Eling TE. Overexpression of 15-lipoxygenase-1 induces growth arrest through phosphorylation of p53 in human colorectal cancer cells. Mol Cancer Res 2005;3:511–7.
[62] Jin HS, Bae SM, Kim YW, Lee JM, Namkoong SE, Han BD, et al. Distinctive cell cycle regulatory protein profiles by adenovirus delivery of p53 in human papillomavirus-associated cancer cells. Int J Gynecol Cancer 2006;16:698–707.
[63] Resnick-Silverman L, Manfredi JJ. Gene-specific mechanisms of p53 transcriptional control and prospects for cancer therapy. J Cell Biochem 2006 [Epub ahead of print].
[64] Tavassoli M, Soltaninia J, Rudnicka J, Mashanyare D, Johnson N, Gaken J. Tamoxifen inhibits the growth of head and neck cancer cells and sensitizes these cells to cisplatin induced-apoptosis: role of TGF-beta. Carcinogenesis 2002;23:1569–75.
[65] Rohlff C, Blagosklonny MV, Kyle E, Kesari A, Kim IY, Zelner DJ, et al. Prostate cancer cell growth inhibition by tamoxifen is associated with inhibition of protein kinase C and induction of 21(waf1/cip1). Prostate 1998;37:51–9.
[66] Ganansia-Leymarie V, Bischoff P, Bergerat JP, Holl V. Signal transduction pathways of taxanes-induced apoptosis. Curr Med Chem Anti-Canc Agents 2003;3:291–306.
[67] Yang HL, Pan JX, Sun L, Yeung SC. p21 Waf-1 (Cip-1) enhances apoptosis induced by manumycin and paclitaxel in anaplastic thyroid cancer cells. J Clin Endocrinol Metab 2003;88:763–72.
[68] Liu W, Zhang R. Upregulation of p21WAF1/CIP1 in human breast cancer cell lines MCF-7 and MDA-MB-468 undergoing apoptosis induced by natural product anticancer drugs 10-hydroxycamptothecin and camptothecin through p53-dependent and independent pathways. Int J Oncol 1998;12:793–804.
[69] Gorospe M, Shack S, Guyton KZ, Samid D, Holbrook NJ. Up-regulation and functional role of p21Waf1/Cip1 during growth arrest of human breast carcinoma MCF-7 cells by phenylacetate. Cell Growth Differ 1996;7:1609–15.
[70] Fernandes-Alnemri T, Litwack G, Alnemri ES. CPP32, a novel human apoptotic protein with homology to Caenorhabditis elegans cell death protein Ced-3 and mammalian interleukin-1 beta-converting enzyme. J Biol Chem 1994;269:30761–4.
[71] Pagano M, Pepperkok R, Verde F, Ansorge W, Draetta G. Cyclin A is required at two points in the human cell cycle. EMBO J 1992;11:961–71.
[72] Lindemann P, Koch A, Degenhardt B, Hause G, Grimm B, Papadopoulos V. A novel *Arabidopsis thaliana* protein is a functional peripheral-type benzodiazepine receptor. Plant Cell Physiol 2004;45:723–33.